Sustainable Pallets from Flexible Multilayer Plastic Waste: A Response Surface and Finite Element Analysis Approach

Fitri Ayu Radini
Research Centre for Polymer Technology, National Research and Innovation Agency

Dwi Novriadi
Research Centre for Polymer Technology, National Research and Innovation Agency

David N. Vicarneltor
Research Centre for Rocket Technology, National Research and Innovation Agency

Ara G. Rizkyta
Research Centre for Rocket Technology, National Research and Innovation Agency

他

https://doi.org/10.5109/7342478

出版情報：Evergreen. 12 (1), pp.594-607, 2025-03. Interdisciplinary Graduate School of Engineering Sciences, Kyushu University, Japan
バージョン：

Sustainable Pallets from Flexible Multilayer Plastic Waste: A Response Surface and Finite Element Analysis Approach

Fitri Ayu Radini[1,*], Dwi Novriadi[1], David N. Vicarneltor[2], Ara G. Rizkyta[2], Annisa Rifathin[1], Zarlina Zainuddin[1], Ade Pratama[1], Ade M. Wijaya[1], Reza Pahlevi Rudianto[1], Riana Y.H. Sinaga[3]

[1]Research Centre for Polymer Technology, National Research and Innovation Agency, B.J. Habibie Science and Technology Area, Building 460, South Tangerang, Banten, Indonesia 15314

[2]Research Centre for Rocket Technology, National Research and Innovation Agency, Jl. Raya Lapan, No. 2, Mekarsari, Rumpin, Bogor, West Java, Indonesia 16350

[3]Research Centre for Sustainable Production System and Life Cycle Assessment, National Research and Innovation Agency, BJ Habibie Science and Technology Area, Building 720 Innovation and Technology Business Centre (Management Building), South Tangerang, Banten, Indonesia 15314

*Author to whom correspondence should be addressed:
E-mail: fitr016@brin.go.id

(Received September 16, 2024; Revised January 3, 2025; Accepted March 5, 2025).

Abstract: Flexible metalized multilayer packaging (MMLP) plastic waste is environmentally challenging due to its various composition and low recycling rate. This study investigates the potential of a blend of MMLP waste, high-density polyethylene (rHDPE) from bottle caps, and polyethylene-glycidyl methacrylate (PE-g-GMA) for pallet products. The blend formulation was optimized for the highest possible compressive elastic modulus using Response Surface Methodology (RSM) and Central Composite Design (CCD). With a ratio of 0.6393 of rHDPE to MMLP and a PE-g-GMA content of 6.7786%, this optimized formulation exhibited a compressive elastic modulus of 190 MPa. The mechanical performance of pallets manufactured from the optimized formulation was predicted using Finite Element Analysis (FEA). The FEA results indicate that the pallet can endure loads up to 600 kg without undergoing permanent plastic deformation. As a result of the weight of 250 kg, the deformation is less than 4 mm, therefore meeting the stiffness performance criteria of the ISO 8611 standard.

Keywords: multilayer plastic waste; pallet; response surface methodology; finite element analysis; solidwork

1. Introduction

Plastic waste is a major global issue, with increasing volumes produced as the global population and living standards rise. According to research by Honingh, plastic waste that pollutes the environment is more likely to cause flooding than organic waste[1)], probably because it cannot decompose naturally[2–4)]. One is flexible metalized multilayer packaging (MMLP) plastic, such as pouches, bags, and shrink films, which covers around 21% and 68% of the plastic waste that pollutes rivers in Java, Indonesia[1,5,6)]. The low recycling rate of Flexible MMLP plastic waste contributes to pollution due to the low value of recycled products, such as garbage bags, buckets, and household items[1,7)]. Developing recycling methods for producing high-value products that may effectively increase the recycling rate of Flexible MMLP plastic waste is essential.

Studies to develop recycling processes for flexible MMLP plastic waste are ongoing and pose a significant challenge as flexible MMLP plastic contains multiple types of plastics, such as polypropylene (PP), polyethylene terephthalate (PET), polyethylene (PE), and aluminum[6)]. These challenges can be overcome by chemically and mechanically recycling flexible MMLP waste. The following involves directly processing MMLP plastic waste in a single material without separating each type of plastic and aluminum in the beginning. The chemical recycling of flexible MMLP plastic waste involves utilizing catalytic or uncatalyzed pyrolysis methods to produce aluminum and petrochemical feedstocks such as oil, gas, and charcoal[8,9)]. However, energy costs prevent this chemical recycling method from being widely deployed. In contrast, mechanical recycling of flexible MMLP plastic waste using the compounding method is preferred because it is much less costly than chemical recycling[10].

Several studies have described the application of compatibilizers in the compounding process of flexible multilayer packaging (MLP) waste to produce polymer blends with favorable physicomechanical performance. According to research by Uehara, using compatibilizers such as PE-g-MA and E-GMA in flexible MLP waste compounds has enhanced their impact strength and elongation at break[11]. Jonkkari added a PE-g-MA compatibilizer to a flexible MLP/LDPE compound, which increased the strain at break and the elastic modulus[12]. The improved mechanical value may be attributable to compatibilizer, which enhances the interfacial bonding between polymeric materials[13]. Nevertheless, studies on using compatibilizers in flexible MMLP compounding are limited.

Compounding flexible MMLP waste with single-layer plastic waste enables the production of panels that can be used to make various recycled products, including pallets[14]. Processing flexible MMLP waste into pallet products may increase the recycling rate of flexible MMLP waste as the plastic pallet production industry is growing, with the global market expected to reach 586 million units by 2027[15]. The growth of the plastic pallet market is likely attributable to the versatile usage of plastic pallets in various industries such as food and beverage, pharmaceutical, automotive, manufacturing, and infrastructure[16]. In addition, plastic pallets provide more design variations since they can be manufactured by injection molding or by utilizing plastic panels through extrusion[17].

One of the most significant performance aspects of a plastic pallet is stiffness. *Pallet stiffness* can be defined as the degree to which a pallet deflects when loaded with goods and measured using its elasticity modulus[18,19]. Pallets will experience deflection while handling goods, whether in racking, stacking, or without racking and stacking conditions and in a static position on the floor or lifted by a forklift. The deflection will appear due to compression loads for pallets intended for handling goods in a static position on the floor without racking and stacking conditions. At the same time, forklifts will give flexural loads[20]. The mechanical properties, such as deflection values, can be measured using actual product testing or Finite Element Analysis (FEA) simulations. The FEA simulation method allows for efficient time and cost savings because there is no need to manufacture and test the actual product[21]. Some authors, such as Baig, Waseem, and Bayona, have conducted research using FEA simulation to predict the performance of pallet products[22–24].

To the author's knowledge, studies on predicting the performance of plastic pallets from flexible MMLP waste have yet to be conducted. The author has discovered Boonsri's research, which estimates the flexural strength and elastic modulus of pallets made from a mixture of MLP waste, HDPE waste, wood powder, and compatibilizer[25]. However, Boonsri's estimation of pallets' mechanical properties is less accurate because it did not go through pallet product testing or FEA simulation. Boonsri also did not optimize the compound composition, which can affect the elastic modulus value[12,26].

Optimization regards the circumstances under which a specific process or technique yields the most favorable outcome. The traditional optimization method is single-variable, focusing on one variable while maintaining the other constant at a time. The drawback of this method is the exclusion of the interacting effects among the examined variables, so it cannot describe the comprehensive effect of all variables on the response. Moreover, it requires more experiments, increasing time, costs, and material consumption[27].

The solution to the above limitations is the application of Response surface methodology (RSM), a multi-variable at a time optimization method. RSM combines mathematical and statistical approaches to predict and optimize responses affected by multiple variables by generating polynomial equations. RSM can describe the effect of each variable and the interaction effect among variables on the response with the fewest experiments[27,28]. RSM also identifies the variables that significantly affect the response[27] . This method assesses the topography of the response surface to identify either a global or local optimal response region (maximum or minimum as needed) utilizing an experimentally designed set of variables[27].

The experiments in RSM can be designed using the CCD (central composite design) or BBD (the box-Behnken design) method. The CCD method is the most widely used and efficient design method because it allows for using two variables. In contrast, the BBD method requires at least three variables, resulting in fewer runs on the CCD[28,29]. RSM and CCD are currently widely used to optimize plastic compounding formulations. Malyuta et al.[30], Dixit et al.[31], and Javier et al.[32] use RSM and CCD to optimize the compounding formulas of thermoplastic polymers (such as PET, PE, and PP) with organic or inorganic filler to achieve desired mechanical properties.

This paper presents the development of a novel sustainable blend of materials for pallet application utilizing flexible metalized multilayer plastic (MMLP) waste, recycled high-density polyethylene (rHDPE) from bottle caps, and PE-g-GMA compatibilizer. The study aimed to formulate an optimum MMLP/rHDPE/PE-g-GMA blend composition for maximum compressive elastic modulus, a mechanical property required for pallet materials, using Response Surface Methodology (RSM) and Central Composite Design (CCD). These statistical techniques also show which of the blend's components significantly influences compressive elastic modulus. In addition to optimization, this study aims to predict the mechanical performance of pallets made from the optimal MMLP/rHDPE/PE-g-GMA blend using Finite Element

Analysis (FEA). FEA conducts virtual testing of pallets under various static loading to evaluate if the pallet material complies with ISO 8611 deformation requirements. The virtual testing also provides data on the maximum load capacity pallet material can withstand before experiencing permanent deformation.

2. Materials and method

2.1 Materials

Post-consumer flexible MMLP shreds and HDPE bottle cap waste flakes (rHDPE) were supplied by PT Tridi Oasis. The types of polymers contained in MMLP samples are PE, PP and PET based on thermal analysis using DSC. Polyethylene-co-glycidyl methacrylate (PE-g-GMA) was purchased from Sigma Aldrich and used as a compatibilizer.

2.2 Compounding Process

The illustration of the MMLP/rHDPE/Pe-g-GMA blend compounding process is shown in Fig. 1. A pre-treatment procedure is used to remove the moisture in the material, which effectively puts the shredded flexible MMLP in an oven at 80 °C for 24 hours. The mixture of shredded flexible MMLP, rHDPE flakes, and PE-g-GMA (MMLP/rHDPE/PE-g-GMA) is compounded using a single screw extruder (Collin type 30x25L/D) with six-barrel zones and temperature values of 180, 200, 220, 235, 245, and 260 °C. This extrusion machine has a 100rpm rotational speed. The MMLP/rHDPE/PE-g-GMA extrudate is then placed in a pelletizer to produce mixed pellets. At least twenty-four hours were spent with the pellets in an oven at 80 °C.

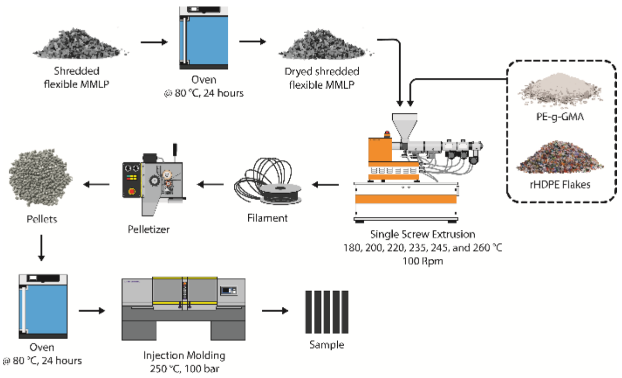

Fig. 1: The compounding process of MMLP/rHDPE/PE-g-GMA blend.

2.3 Experimental Design

As the statistical method, Response Surface Methodology (RSM) was implemented in this study to optimize the MMLP/rHDPE/PE-g-GMA compound formulation for maximum compressive elastic modulus. The Central Composite Design (CCD), one of the RSM experimental designs, has been applied with variables: the weight ratio of rHDPE to MMLP (P) and PE-g-GMA percentage to the total weight of polymer (C). The observed response was compression elastic modulus (CM).

The CCD with variables P and C has 11 randomized runs experiment that consists of 4 factorial runs, 3 replication runs of the center point, and 4 axial points run. Each variable has five levels in coded value, which is ± 1 for high and low level (factorial run), 0 for mid-level (center point run) and ± 1.414 for extreme high and low level (axial point run)[29]. The dimensionless coded value is needed for computational efficiency. The variables P and C are expressed in the actual unit, and Eq. 1) is used to convert the actual unit of variables P and C into coded values. Table 1 shows the variables P and C at five levels in coded value and actual unit.

The present research uses the rsm package in Rstudio software. The function coded.data in the rsm package is used to convert the actual unit of the variable into coded value, and the function decode.data does the opposite. Meanwhile, the ccd function in the rsm package is used to generate the experimental design.

Table 1. Design of experiment

Variables	Symbol	Level of variables				
		-1.41	-1	0	+1	+1.41
Ratio rHDPE/MMLP	P	0.16	0.3	0.65	1	1.14
%wt PE-g-GMA	C	0.34	2	6	10	11.65

$$x_1=\frac{P-0.65}{0.35}\ ;\ x_2=\frac{C-6}{4} \qquad (1)$$

2.4 Compressive Test

Sample testing preparation was carried out using an injection molding machine. As much as 1 kg of MMLP/rHDPE/PE-g-GMA pellets was injected into a rectangular mold with a size of 12.7 x 3.2 x 100 mm³ using a Battenfeld BA 400 CDC injection molding machine with a heating temperature of 220 – 250 °C and a cooling time of 20 s. After the injection, the sample was manually cut and conditioned in a room with a temperature of 23 ± 2 °C and 50% humidity for more than 40 hours before testing.

A universal testing machine (UTM) with a load cell of 50 kN is used to measure the sample's compressive strength and compressive elastic modulus. Each sample consists of five specimens with a size of 12.7 x 3.2 x 100 mm³ with a pressing speed of 1.3 mm/min and a distance between grips of 12.7 mm. The sample area exposed to compressive load is 12.7 x 3.2 cm². Apart from UTM, sensors (strain gauges) are also used on both sides of the specimen to determine the Poisson ratio in the sample. Fig. 2 represents an illustration of the compression test, demonstrating the measurement of lateral strain to determine Poisson's ratio. The compression test results will be used to create a static loading simulation.

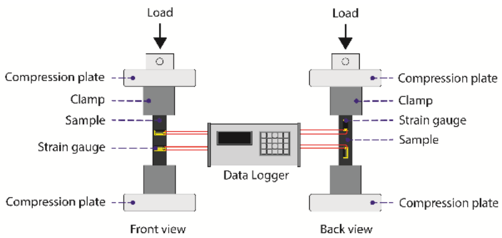

Fig. 2: The compression test schematic.

2.5 Mathematical modelling, statistical analysis and optimization

The second-order regression model is built using Rstudio software with the rsm function and several additional functions, such as the FO function for linear terms, the TWI function for the two-way interaction terms and the PQ function for pure quadratic terms. This function also results in ANOVA tables for statistical analysis and stationary points for predicting the optimized variables (P and C) for maximum compression elastic modulus (CM). Meanwhile, the 2D contour and 3D surface plots are produced using the contour and persp function[33].

2.6 FEA pre-processing

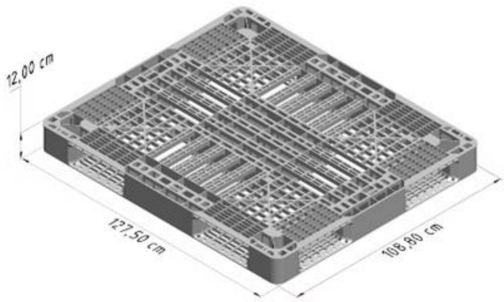

(a)

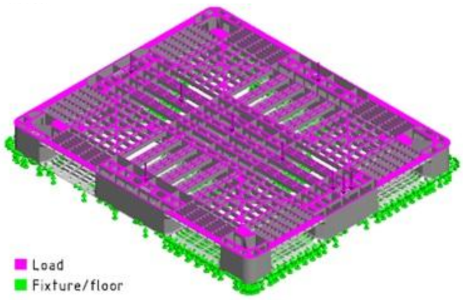

(b)

Fig. 3: Commercial pallet design (a) pallet dimension, (b) boundary condition.

FEA is performed using SolidWorks software based on the material properties of the optimum compressive elastic modulus formulation of MMLP/rHDPE/PE-g-GMA to predict the performance of the pallet. A commercial pallet design with dimensions of 127.5×108.8×12 cm3 and a rib thickness of 1.5–2.0 mm is used as a reference, as shown in Fig. 3(a). In this simulation, static load is given to the upper surface of the pallet while it is on the floor (Fig. 3(b)), with load variations of 100 kg to 1000 kg with intervals of 100 kg. In addition, a convergence test is performed to see the stability of the maximum stress with an error of less than 7% of the mesh size[34]. Figure 4 is the result of the convergence test, with a mesh size of 2–10 mm with an interval of 1 mm. The findings indicated that the mesh size within the tested range did not yield a significant variance[35]. Therefore, this study employed a tetrahedral mesh with a 10 mm size to optimize computational efficiency. The results of this FEA are in the form of a distribution of maximum von Mises stress, safety factor and deflection due to the loading that occurs.

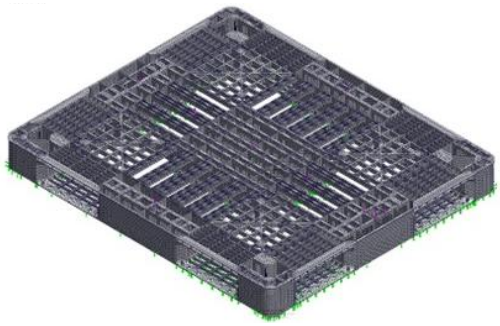

(a)

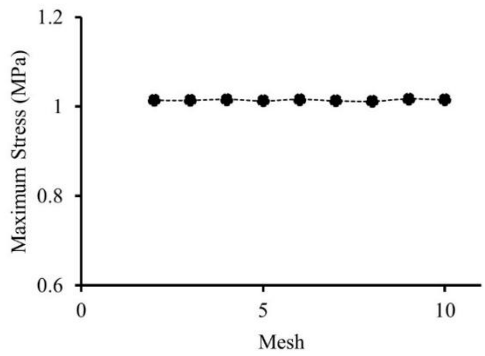

(b)

Fig. 4: (a) Mesh size, (b) Convergence test result

2.7 FTIR Testing

This study utilizes FTIR testing to compare the chemical functional groups observed in the highest and the lowest compressive elastic modulus samples. Testing occurred using a Bruker Alpha II FTIR spectrometer with the following parameters: attenuated total reflection (ATR) technique, wavenumber range of 4000 to 600 cm^{-1}, and a scan frequency of 32 scans per minute. The test sample was a thin section cutting from the compression test specimen.

3. Results and discussion

3.1 Process analysis

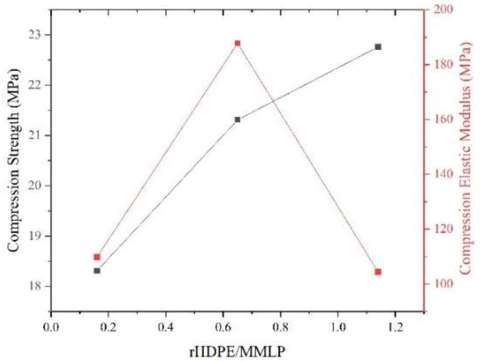

Fig. 5: Effect of ratio rHDPE/MMLP on compression elastic modulus and compression strength of MMLP/rHDPE/PE-g-GMA compound.

Figure 5 depicts the effect of the rHDPE/MMLP ratio on the Compression Elastic Modulus and Compression Strength. It can be observed that the increment of the rHDPE/MMLP ratio, from 0.16 to 0.65, increased the compression elastic modulus by 70.99%. However, at the 1.14 ratio of rHDPE/MMLP, compression elastic modulus is relatively decreased by 4.93%. The increment of the rHDPE/MMLP ratio from 0.16 to 0.65 and 1.14 increased the compression strength by 16.39% and 24.31%.

At the 0.16 ratio, weak interfacial adhesion between recycled MMLP and rHDPE may occur at high MMLP content, resulting in defects like interfacial debonding lowering the compression strength and elastic modulus value. This phenomenon is consistent with Boonsri's work with recycled plastic waste, with an increment of flexural strength and elastic modulus at 10% plastic waste content but decreasing at 15% and 20%[25]. The same thing could occur with MMLP and HDPE composites.

MMLP used in this research consists of various layers such as PE, PP, PET and Aluminum. According to Boonsri, a certain quantity of plastic waste addition can act as filler reinforcement in the matrix, making it stiffer. This increase may have occurred due to plastic waste was partially melted because of manufacturing temperatures that were lower than the crystalline melting temperatures of PET[25]. The compressive strength and elastic modulus increment at the 0.65 ratio were affected by the unmelted MMLP. However, it did not cause defects such as interfacial debonding, so it acted as a filler and reinforced the composite. It is hypothesized that MMLP is more elastic than rHDPE, increasing stiffness and accumulating intermolecular stresses, resulting in a rise in compression strength and elastic modulus.

The compression strength is increased at the 1.14 ratio due to the high content of rHDPE, which results in better adhesion, plus with the reinforcement of MMLP. The decreased compression elastic modulus at 1.14 ratio was assumed to be caused by lower MMLP content, which means lower filler content, thus decreasing the rigidity of the composite. This mechanism made rHDPE properties more dominant, which is more plastic, and resulted in a more extended strain, which lowered the elastic modulus value.

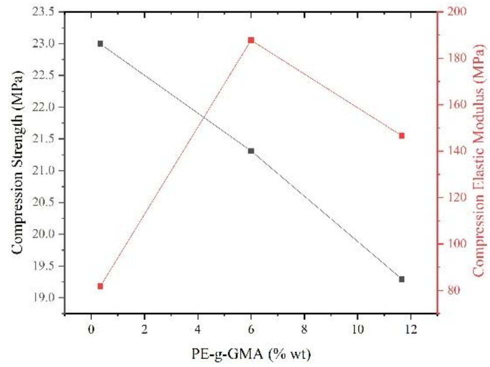

Fig. 6: Effect of %wt PE-g-GMA on compression elastic modulus and compression strength of MMLP/rHDPE/PE-g-GMA compound.

PE-g-GMA was added to the blend to increase adhesion between the rHDPE and MMLP. The enhanced interfacial adhesion between rHDPE and MMLP is thought to positively influence stress transmission, reducing the likelihood of interfacial debonding and improving compression properties. The following is similar to what occurred with LDPE and corn starch blends[36].

Figure 6 depicts the effect of PE-g-GMA content on the Compression Elastic Modulus and Compression Strength. It can be observed that the increment of PE-g-GMA content, from 0.34 % to 6%, increased the compression elastic modulus by 129.77% and at 11.66% content, the compression elastic modulus increased by 79.47%. For compression strength, the increment of PE-g-GMA content from 0.34% to 6% decrease the compression strength by 7.33%, and a further increment to 11.66% of PE-g-GMA decrease the compression strength by 16.1%.

The elastic modulus result shows some compressive strain decreases with increasing PE-g-GMA, implying that PE-g-GMA makes the composite more elastic. The above could be due to improved adhesion between rHDPE and MMLP, which increases the stiffness of the blend. The decrease in compression strength with increasing compatibilizer content could be attributable to too much compatibilizer migrating around the MMLP, creating self-entanglement among the compatibilizers rather than the rHDPE, resulting in slippage.

3.2 RSM statistical analysis

This study uses FEA to predict the stiffness of a pallet made of MMLP/rHDPE/PE-g-GMA material in a static position on the floor without racking and stacking conditions. The stiffness of the pallet is measured in terms of the material's elastic modulus. In addition, pallets in a static position on the floor without racking and stacking conditions are subjected to compression loads. Thus, the compressive elastic modulus of the MMLP/rHDPE/PE-g-

GMA blend material was evaluated and statistically optimized using Rstudio.

The compressive elastic modulus (CM) of MMLP/rHDPE/PE-g-GMA blend material obtained from the eleven CCD experiments in Table 2 was used to develop an RSM model expressed as a coded variable in Rstudio software. The RSM-coded model presented in Eq. 2 is a second-order polynomials equation composed of a first-order or linear term (FO), the interaction between variables (TWI), and pure quadratic or squared terms (PQ). In addition, X1 is the code symbol of the variable weight ratio of rHDPE to MMLP (P), and X2 is the code symbol of the variable percentage of PE-g-GMA to total polymer weight (C).

$$CM\ (MPa) = 187.7907 - 2.4728\ X1 + 14.3829\ X2 - 2.5703\ X1\ X2 - 40.4874\ X1^2 - 36.9460\ X2^2 \quad (2)$$

A good model should be capable of predicting compressive elastic modulus (CM) values that best fit the experimental results. Table 3 displays R studio software's ANOVA analysis of Eq. 2. Model Eq. 2 has a p-value < 0.05, R-squared > 0.8, and Adj R-square > 0.8[37–40]. However, the Lack of Fit (LOF) is significant (p-value < 0.05), thus failing to meet the statistical requirements for a good model[38,40,41].

Table 2. Experimental and predicted value of compression elastic modulus (CM).

Run	Coded Variables		Experimental Response	Predicted Response
	X1	X2	CM (MPa)	CM (MPa)
1	-1	1	121.46	127.22
2	0	0	190.86	187.79
3	-1	-1	104.71	98.45
4	+1	+1	110.26	122.27
5	+1	-1	103.79	93.50
6	0	0	185.23	187.79
7	0	0	187.28	187.79
8	0	+1.41	146.67	134.24
9	+1.41	0	104.41	103.32
10	-1.41	0	109.82	110.31
11	0	-1.41	81.73	93.56

Table 3. The analysis of variance (ANOVA) parameter of CM model Eq. 2.

Source	Terms	Multiple R^2	Adj R^2	p - value	F - value
Model		0.9607	0.9214	0.001595	24.44
Intercept				8.40e-07	
FO (X1, X2)				0.0354	7.0034
	X1			0.5538	
	X2			0.0141	
TWI (X1, X2)				0.6607	0.2172
	X1: X2			0.6607	
PQ (X1, X2)				0.00041	53.9769
	$X1^2$			0.0003278	
	$X2^2$			0.0005045	
Lack of Fit (LOF)				0.0398	

Eliminating non-significant model terms, with p-value > 0.05 and F-value < 4, produces an insignificant lack of fit[38]. The interaction term between variables, TWI, has a p-value of 0.66 and an F-value of 0.21. Hence, TWI is removed from the Eq. 2 to build a more accurate model for predicting CM values. Eq. 3 shows the RSM model in code units after removing terms that do not significantly affect response.

$$CM\ (MPa) = 187.7907 - 2.4728\ X1 + 14.3829\ X2 - 40.4874\ X1^2 - 36.9460\ X2^2 \quad (3)$$

The model represented by Eq. 3 has a p-value of 0.0002677, an F-value of 35.06, R-square and Adj R-square values of 0.959 and 0.9316, respectively, and an insignificant lack of fit (p-value 0.05056). Therefore, Eq. 3 has shown to be a reliable model for predicting the value of the compressive elastic modulus of the MMLP/rHDPE/PE-g-GMA composite[41], as long as the composition is in the boundaries that have been made. Eq. 4 contains the uncoded or actual variables of the model stated in Eq. 3.

$$CM\ (MPa) = -51.9600 + 422.5969\ P + 31.3052\ C - 330.5092\ P^2 - 2.3091\ C^2 \quad (4)$$

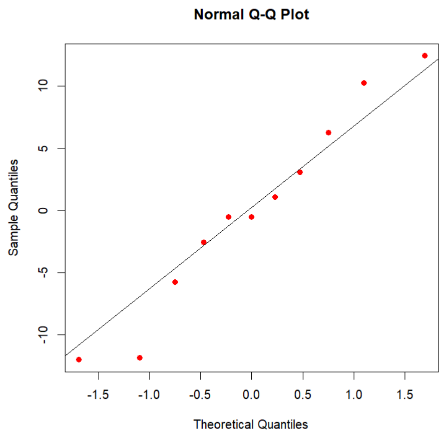

(a)

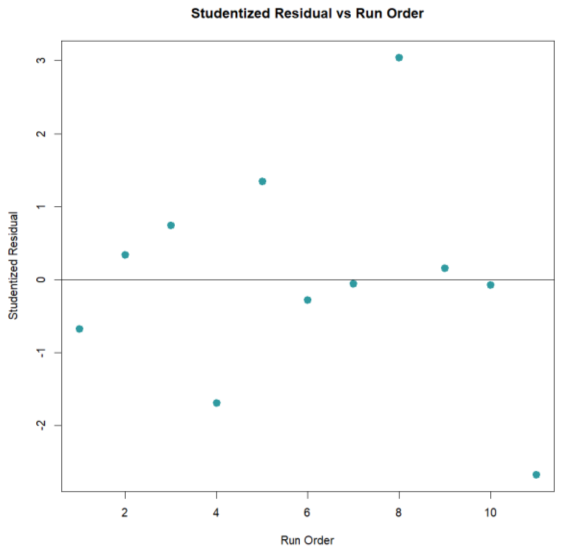

(b)

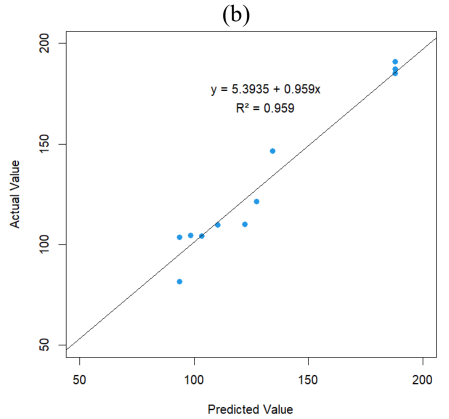

(c)

Fig. 7: (a)Normal plot of residual for CM model, (b)Residual vs run order plot for CM model, (c) The plot of actual vs. predicted CM values.

The validity of the model Eq. 3 was further investigated using residual analysis plots and the predicted vs actual plot. Figure 7(a) shows that the plot follows a linear pattern, which suggests that the data follow the normal probability distribution[42,43]. Residual data in Fig. 7(b) randomly distributed with no apparent trends are found. The actual and predicted CM values show a linear curve fit relationship with an R^2 value closer to 1.0, as shown in Fig. 7(c), reflecting the best fit and acceptable agreement between the actual and predicted values. The findings presented here demonstrate that the model in Eq. 3 is suitable for illustrating the relationship between the formulation variables, namely the ratio of rHDPE to MMLP (X1) and the percentage of weight PE-g-GMA (X2), with the response compression elastic modulus (CM)[44] . Furthermore, this model can be utilised to determine the optimal compressive elastic modulus of the MMLP/rHDPE/PE-g-GMA blend.

The analysis of variance (ANOVA) also helps determine whether or not a given term variable has a significant influence. The p-value determines the significance of a variable's contribution to the response value[45]. The smaller the p-value, the more significant the contribution. Variables with a p-value above 0.05 indicate an insignificant contribution to the response value[46].

Table 3 reveals that the variable that contributes most to the CM response is $X1^2$, the quadratic terms of the rHDPE to MMLP ratio. The second variable contributing to the CM response is $X2^2$ or the quadratic terms of %wt PE-g-GMA. These quadratic terms significantly contribute to the CM response, indicating that the rHDPE to MMLP ratio and %wt PE-g-GMA variable affect CM non-linearly. The linear term of %wt PE-g-GMA variable is also significant because having a p-value below 0.05. However, the p-value of linear %wt PE-g-GMA variable is still higher than the quadratic term, indicating that the quadratic term contributes more to CM response. Meanwhile, the CM response is unaffected by the linear terms of variable X1 and the interaction terms. Therefore, Figure 8 shows the nonlinear influence of rHDPE to MMLP ratio and %wt PE-g-GMA on the CM response of the MMLP/rHDPE/PE-g-GMA compound.

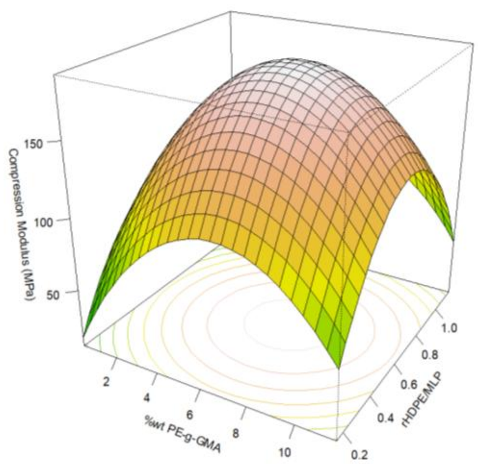

Fig. 8: 3D surface plot for compression elastic modulus of MMLP/rHDPE/PE-g-GMA.

The correlation between the formulation variables, ratio rHDPE/MMLP (X1) and %wt PE-g-GMA (X2), with the response compression elastic modulus (CM) in Eq. 3 is presented in three-dimensional response plots, as shown in Fig. 8. According to Fig. 8, the addition of rHDPE/MMLP at a ratio of 0.16 to 0.65 increases the compressive elastic modulus up to an optimum point and then decreases as the rHDPE/MMLP ratio increases. Favaro also reported that PE-based elastic modulus gets the optimum point with the addition of MLP then decreased with increasing MLP ratio[47]. 3D surface curve plot also shows the significant condition of the %compatibilizer to increase the compressive elastic modulus with a value of 0.34% to 6% then decrease as the %compatibilizer ratio increases. The results are aligned with Fig. 5 and 6.

Optimization produces the maximum compressive elastic modulus (CM) response value. The 2D contour plot image of the compressive elastic modulus of the MMLP/rHDPE/PE-g-GMA compound can predict the optimum formulation region. The range with the highest CM response value corresponds to the lightest part on the contour plot. Figure 9 demonstrates that the maximum achievable CM is above 180 MPa with the optimum formulation range of rHDPE/MMLP ratio 0.6 – 0.7 and PE-g-GMA 6 – 7 wt%.

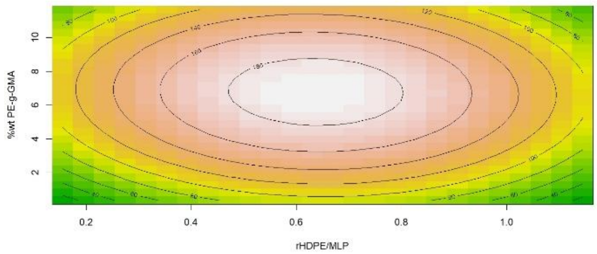

Fig. 9: 2D Ccontour plot for compression elastic modulus of MMLP/rHDPE/PE-g-GMA.

RSM analysis utilizing the Rstudio generates stationary points derived from the mathematical response prediction model, which indicates the optimal formulation's estimation. In code units, the optimal formulation prediction based on Eq. 3 is -0.0305 for X1 and 0.1946 for X2. Meanwhile, in actual units, the rHDPE/MLP ratio is 0.6393, and PE-g-GMA is 6.7786 wt%. As seen in Fig. 9, the predictions fall within the prediction range of the optimal formulation.

Inserting the unit code stationary point into the following Rstudio software function yielded the maximum predicted CM value:

```
max<-data.frame(x1=-0.0305,x2=0.1946)
predict(e modulus,max)
```

The maximum CM prediction value is 189.2282 MPa. A verification experiment took place on the optimal formulation (with an rHDPE/MLP ratio of 0.6393 and a PE-g-GMA content of 6.7786 wt%) to validate the Eq. 3 model and the predicted maximum CM value. The verification sample's CM value was 190 MPa. The difference between the predicted and actual verification maximum CM values has a 2% error. Therefore, an error value is within the allowable range of 5%, confirming that the prediction model in Eq. 3 is 95% accurate in CM prediction[48].

3.3 FEA post-processing

In this study, FEA was conducted to evaluate the mechanical performance of pallets at various load levels under static conditions on the floor without stacking and racking. In FEA, the optimum MMLP/rHDPE/PE-g-GMA verification results were used as material parameters consisting of density, compressive strength, compressive elastic modulus, and Poisson's ratio, as shown in Table 4.

Table 4. MMLP/rHDPE/PE-g-GMA material properties for FEA Simulation.

Properties	Unit
Density	940.1 Kg/cm3
Compressive elastic modulus	193.234 MPa
Compressive strength	18.827 MPa
Poisson ratio	0.4
Yield strength	6.06541 MPa

The FEA output was selected using the Von Mises criterion to predict the permanent deformation of the pallet material. If the von Mises stress exceeds the yield strength, the pallet is predicted to undergo plastic deformation, where it experiences functional failure[49]. The criteria selection is based on the characteristics of ductile plastic materials, which tend to experience plastic deformation before breaking[50]. In addition, this criterion is also known as Distortion Energy Theory[49], which is considered more accurate in predicting when isotropic materials such as plastics will experience plasticity under multi-axial loading conditions, which often occur in pallet applications.

The FEA results (Fig. 10) show similar stress distribution patterns throughout the pallet model, regardless of the applied load variations. The stress distribution in the pallet model is dominated by blue contours and green on the unsupported part. The red contour is on the bottom of the upper surface floor of the pallet with nodes 229499, shown in Fig. 11. The maximum stress value on the red contour increases significantly with increasing load.

The results of the FEA in terms of von Mises stress value at different compression loads are shown in Table 5. At 100 kg, the stress is only 1.025 MPa, but this increases to 9.886 MPa at 1000 kg. Compared to the material yield stress value of 6.06541 MPa, such von Mises stress values show that the pallet material starts to experience plastic deformation at a load of about 700 kg. Above that load, the pallet goes into a critical state where it becomes permanently deformed, possibly resulting in structural failure[49].

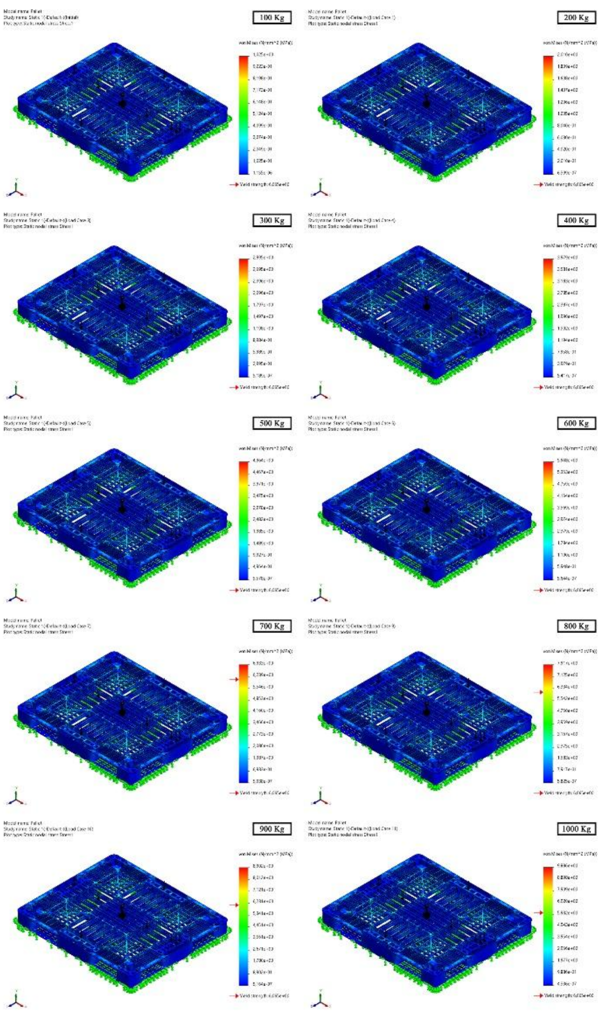

Fig. 10: Von mises stress distribution FEA of 100 – 1000 Kg load.

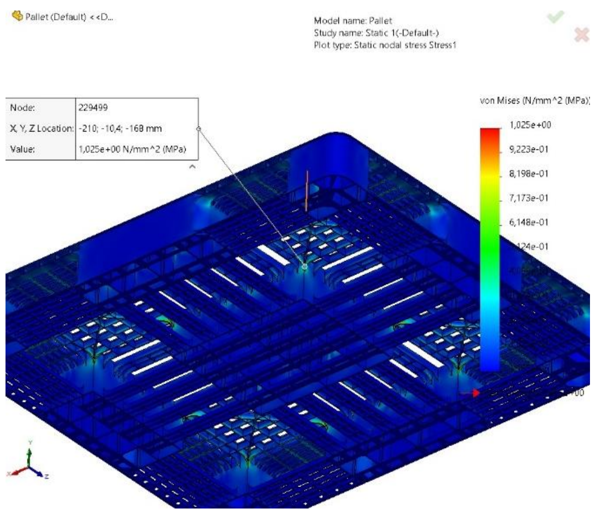

Fig. 11: Maximum stress probe location of pallet.

Table 5. von Mises stress and deflection from FEA.

Load (Kg)	Stress (MPa)		Deflection (mm)	
	Min	Max	Min	Max
100	$1.155e^{-6}$	1.025	$1.000\ e^{-30}$	1.675
200	$6.599e^{-7}$	2.010	$1.000\ e^{-30}$	3.282
300	$5.189e^{-7}$	2.995	$1.000\ e^{-30}$	4.889
400	$5.417e^{-7}$	3.979	$1.000\ e^{-30}$	6.496
500	$5.578e^{-7}$	4.964	$1.000\ e^{-30}$	8.103
600	$5.644e^{-7}$	5.948	$1.000\ e^{-30}$	9.71
700	$5.938e^{-7}$	6.933	$1.000\ e^{-30}$	11.32
800	$5.825e^{-7}$	7.917	$1.000\ e^{-30}$	12.92
900	$5.164e^{-7}$	8.902	$1.000\ e^{-30}$	14.53
1000	$4.536e^{-7}$	9.886	$1.000\ e^{-30}$	16.14

Figure 12 shows the safety factor (FOS) generated by FEA. At 100 kg, the resulting FOS is 5.919, indicating that the pallet has sufficient capacity to withstand the load without risk of failure. However, the FOS value decreases drastically as the load increases, reaching 0.6135 at 1000 kg. The FOS was defined as the material's yield strength ratio to the maximal von Mises stress[51]. FOS less than one is recorded when the pallet is subjected to a load above 600 kg, indicating that the stress experienced by the pallet has exceeded the yield strength of the optimum MMLP/rHDPE/PE-g-GMA material. This low FOS value indicates that the pallet is in a critical condition, where structural failure can occur at any time if the load increases[22,51]. Consequently, the maximum load capacity for the pallet should not exceed 600 kg to minimize the risk of material failure.

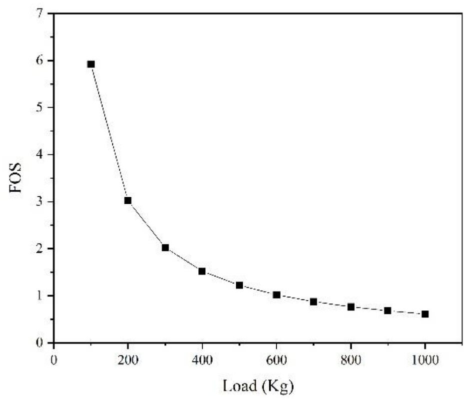

Fig. 12: FOS result of FEA simulation.

In addition to stress, an analysis of the deformation on the pallet was also carried out. The FEA results in Table 5 show an increase in deformation from 1.675 mm at a load of 100 kg to 16.14 mm at a load of 1000 kg. According to the pallet testing standard ISO 8611, the maximum deformation allowed for pallets is 4 mm to ensure stability and safety[20]. The analysis results show that the pallet exceeds the deformation limit set in the 200 kg to 300 kg with deformations of 3.282 mm and 4.889 mm, respectively.

The extensive load range necessitated additional testing at 225 kg, 250 kg, and 275 kg to yield more precise results. In the additional test, 3.684 mm, 4.086 mm, and 4.487 mm deformations were obtained, respectively, as shown in Table 6. Based on the additional data provided, it can be inferred that the maximum load the pallet can withstand without exceeding the deformation limit specified by ISO 8611 is 250 kg. Although the deformation at this load is 4.086 mm or slightly exceeds the standard limit, it can still be considered close to the acceptable threshold. Therefore, to maintain the shape and stability of the pallet structure and prevent structural failure due to excessive deformation, the operational load on the pallet should not exceed 250 kg. Exceeding the load limit of pallets to 250 kg may lead to significant pallet deformation, potentially compromising structural integrity and increasing the likelihood of damage during handling and transportation[52)]. Additionally, continuous use above the recommended load could accelerate wear and tear, shortening the lifespan of the pallet and ultimately leading to higher replacement costs[51)].

Table 6. FEA result for 225 – 275 kg load.

Load (Kg)	Stress (MPa)		Deflection (mm)	
	Min	Max	Min	Max
225	$6.138e^{-7}$	2.256	$1.000\ e^{-30}$	3.684
250	$5.800e^{-7}$	2.502	$1.000\ e^{-30}$	4.086
275	$5.539e^{-7}$	2.748	$1.000\ e^{-30}$	4.487

Through the FEA simulation that has been done, it can be concluded that although the pallet stress distribution remains consistent at each load variation, there are clear operational limitations that must be considered. Based on the von Mises stress and FOS values generated from the FEA simulation, the maximum load the pallet can withstand before plastic deformation is 600 kg because it has a von Mises stress value below the yield stress and an FOS value above 1. However, ISO 8611 provides a maximum deflection requirement for pallet stiffness performance of 4 mm, where this deflection value is obtained in pallets with loads below 600 kg, more precisely at a load of 250 kg. Therefore, the recommended maximum load for pallets with MMLP/rHDPE/PE-g-GMA optimum material is 250 kg for having required deflection of stiffness performance, even though the pallets' mechanical properties can still withstand loads up to 600 kg before fatal structural and material failure.

In order to minimize deflection, the dimensions of the pallet's reinforcing rib can be adjusted without changing the material. However, this adjustment can affect the product's aesthetics and the manufacturing process's effectiveness[52)]. Therefore, further studies are needed to determine the appropriate pallet design for MMLP/rHDPE/PE-g-MA materials.

3.4 FTIR Measurement

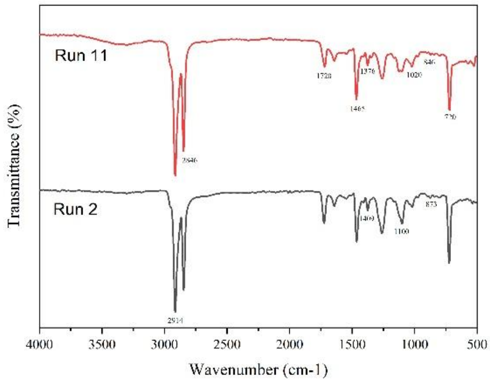

Fig. 13: FTIR spectra of run 2 and run 11 samples.

Figure 13 shows the FTIR spectra of sample run 2 (highest compressive elastic modulus) and sample run 11 (lowest compressive elastic modulus). Both samples exhibit the characteristic peaks of polyethylene (PE), polypropylene (PP), polyethylene terephthalate (PET), and glycidyl methacrylate (GMA).

The characteristic peaks of PE appear at wave numbers 2914 and 2846 cm^{-1}, corresponding to methylene's asymmetric and symmetric stretching vibrations (-CH_2-)[53)]. Additionally, peaks at 1463 – 1465 cm^{-1} indicate bending deformation of methylene groups[53)] , while those at 720 - 724 cm^{-1} represent CH_2 rocking in PE[54)]. The characteristic peak of PP exists at wave number 2914 cm^{-1}, corresponding to the CH_2 asymmetric C-H stretching[53)], and at 1374 - 1376 cm^{-1}, associated with the CH_3 symmetric bending[53)]. The characteristic peaks of PET occur at wave numbers 1719-1723 cm^{-1}, corresponding to C=O stretching of an ester carboxyl group[55)], 1409-1411 cm^{-1}, associated with a para-substituted benzene ring[55)], 1100-1102 cm^{-1}, indicative of O-CH_2 stretching[55)], and 1019-1021 cm^{-1}, related to ring C-H in-plane bending[55)]. GMA exhibits peaks at wave numbers 846 and 873 cm^{-1}, corresponding to the epoxy groups of GMA[56,57)]. Figure 13 indicates no significant difference in FTIR peaks between the sample exhibiting the highest compressive modulus and the sample displaying the lowest. The result demonstrates that the compressive modulus is more affected by the blend composition of the sample than by the chemical functional groups present.

4. Conclusion

This study successfully developed a sustainable material blend for pallet applications using waste MMLP, recycled HDPE, and a PE-g-GMA compatibilizer. The first goal of this study was achieved using the statistical tools Response Surface Methodology (RSM) and Central Composite Design (CCD), resulting in an optimal formulation of MMLP/rHDPE/PE-g-GMA blend with a rHDPE/MMLP ratio of 0.6393 and a PE-g-GMA content of 6.7786%. This optimum formulation produced a compressive elastic modulus of 190 MPa with a validation error of only 2%, demonstrating the accuracy and reliability of the optimization process. The statistical analysis also revealed that the effect of the rHDPE to MMLP ratio on the compressive elastic modulus of the blend is more significant than the PE-g-GMA percentage. In addition, the interaction between the PE-g-GMA percentage and the ratio of rHDPE to MMLP has no significant effect on the compressive elastic modulus of the blend.

The second goal was accomplished using Finite Element Analysis (FEA). FEA test revealed that the pallet manufactured from the optimal blend of MMLP/rHDPE/PE-g-GMA can resist a maximum load of 600 kg before permanent deformation occurs. In comparison, to meet ISO 8611 standards, a maximum operational load of 250 kg is recommended, leading to a 4.086 mm deflection. The result demonstrates the feasibility of the optimized MMLP/rHDPE/PE-g-GMA material blend for pallet lightweight industrial uses.

However, this study primarily focuses on static loading without stacking and racking conditions and simplified pallet design without addressing dynamic loading, impact resistance, and long-term durability.

In order to increase load capacity and improve performance, future research should focus on refining the structural design of the pallet, particularly the rib configuration, to increase load-bearing capacity and minimize deflection under various load conditions. In addition, continued testing for dynamic loads under both stacking and racking conditions and impact resistance is essential to simulate actual conditions to ensure the reliability and durability of the pallet.

Acknowledgements

The authors acknowledge the Research Center for Appropriate Technology Program of The Research Organization of Agriculture and Food - BRIN for funding this research, the facilities support from Polymer Technology Laboratories – BRIN through E-Layanan Sains, material support from PT Tridi Oasis and Kushendarsyah Saptaji from Sampoerna University for giving critical revision on the manuscript.

Nomenclature

MMLP	flexible metalized multilayer packaging
PE-g-GMA	polyethylene-glycidyl methacrylate
RSM	Response Surface Methodology
CCD	Central Composite Design
FEA	Finite Element Analysis
°C	Degrees Celsius
rpm	Revolution per minute
kg	kilogram
mm	Millimeter
s	second
kN	kilonewton
TWI	two way interaction
PQ	Pure quadratic
FO	First Order
Anova	Analysis of Variance
LOF	Lack of Fit
FOS	Factor of Safety

References

1) D. Honingh, T. van Emmerik, W. Uijttewaal, H. Kardhana, O. Hoes, and N. van de Giesen, "Urban river water level increase through plastic waste accumulation at a rack structure," *Front Earth Sci (Lausanne)*, 8 (*February*) 1–8 (2020). doi:10.3389/feart.2020.00028.
2) A. Zhumadilova, and S. Zhigitova, "Features of modern areas of solid waste disposal," *Evergreen*, 10 (*2*) 640–648 (2023). doi:10.5109/7183318.
3) R. Lestari, T.D. Wahyuningsih, and I. Kartini, "High quantum yield nitrogen-carbon dots (n-cds) from plastic waste," *Evergreen*, 10 (*3*) 1313–1322 (2023). doi:10.5109/7151677.
4) M.A. Widyatmika, and N.B. Bolia, "Unveiling segregation and composting behavior in urban communities: a study case of sarbagita municipality, indonesia," *Evergreen*, 11 (*2*) 612–623 (2024). doi:10.5109/7183318.
5) T. Van Emmerik, M. Loozen, K. Van Oeveren, F. Buschman, and G. Prinsen, "Riverine plastic emission from jakarta into the ocean," *Environmental Research Letters*, 14 (*8*) (2019). doi:10.1088/1748-9326/ab30e8.
6) S. Ügdüler, T. De Somer, K.M. Van Geem, M. Roosen, A. Kulawig, R. Leineweber, and S. De Meester, "Towards a better understanding of delamination of multilayer flexible packaging films by carboxylic acids," *ChemSusChem*, 14 (*19*) 4198–4213 (2021). doi:10.1002/cssc.202002877.
7) R.A. Muñoz Meneses, G. Cabrera-Papamija, F. Machuca-Martínez, L.A. Rodríguez, J.E. Diosa, and E. Mosquera-Vargas, "Plastic recycling and their use as raw material for the synthesis of carbonaceous materials," *Heliyon*, 8 (*3*) (2022). doi:10.1016/j.heliyon.2022.e09028.
8) K. Sivagami, G. Divyapriya, R. Selvaraj, P. Madhiyazhagan, N. Sriram, and I. Nambi, "Catalytic pyrolysis of polyolefin and multilayer packaging based waste plastics: a pilot scale study," *Process Safety and Environmental Protection*, 149 497–506 (2021). doi:10.1016/j.psep.2020.10.038.
9) S. Yin, R. Rajarao, B. Gong, Y. Wang, C. Kong, and V. Sahajwalla, "Thermo-delamination of metallised composite plastic: an innovative approach to generate aluminium from packaging plastic waste," *J Clean*

Prod, 211 321–329 (2019). doi:10.1016/j.jclepro.2018.11.158.
10) C.T. de M. Soares, M. Ek, E. Östmark, M. Gällstedt, and S. Karlsson, "Recycling of multi-material multilayer plastic packaging: current trends and future scenarios," *Resour Conserv Recycl*, 176 (*June 2021*) (2022). doi:10.1016/j.resconrec.2021.105905.
11) G.A. Uehara, M.P. França, and S. V Canevarolo Junior, "Recycling assessment of multilayer flexible packaging films using design of experiments," *Polimeros*, 25 (*4*) 371–381 (2015). doi:10.1590/0104-1428.1965.
12) I. Jönkkäri, V. Poliakova, V. Mylläri, R. Anderson, M. Andersson, and J. Vuorinen, "Compounding and characterization of recycled multilayer plastic films," *J Appl Polym Sci*, 137 (*37*) (2020). doi:10.1002/app.49101.
13) S. Singh, L. Nagdeve, H. Kumar, and K. Dhakar, "Rice straw based natural fiber reinforced polymer for sustainable bio-composites: a systematic review," *Evergreen*, 10 (*2*) 1041–1052 (2023). doi:10.5109/6793661.
14) P. Soemadijo, F. Anindita, D. Trisyanti, R. Akib, M. Abdulkadir, N.M. Nizardo, and R.L. Rachmawati, "A study of available technology for recycling low value plastic in indonesia," *Journal of Environmental Science and Sustainable Development*, 5 (*2*) 436–457 (2022). doi:10.7454/jessd.v5i2.1128.
15) Madhumitha Jaganmohan, "Global plastic pallets market volume 2018 & 2027," *Https://Www.Statista.Com/Statistics/971747/Global-Plastic-Pallets-Market-Size/*, (2019). https://www.statista.com/statistics/971747/global-plastic-pallets-market-size/.
16) C. Chama, K. Harding, J. Mulopo, and P. Chego, "A multi-criteria decision analysis approach to pallet selection: development of a material-of-construction evaluation model," *South African Journal of Industrial Engineering*, 32 (*3*) 52–64 (2021). doi:10.7166/32-3-2614.
17) I. Deviatkin, and M. Horttanainen, "Carbon footprint of an eur-sized wooden and a plastic pallet," *E3S Web of Conferences*, 158 1–7 (2020). doi:10.1051/e3sconf/202015803001.
18) T. You, and J.K. Eom, "A simple regression approach to the shortened stiffness tests for pallets," *International Journal of Advanced Logistics*, 3 (*1–2*) 55–74 (2014). doi:10.1080/2287108x.2014.958284.
19) R.H. Alasfar, S. Ahzi, N. Barth, V. Kochkodan, M. Khraisheh, and M. Koç, "A review on the modeling of the elastic modulus and yield stress of polymers and polymer nanocomposites: effect of temperature, loading rate and porosity," *Polymers (Basel)*, 14 (*3*) (2022). doi:10.3390/polym14030360.
20) International Organization for Standardization., "ISO/ts 8611-2:2005(e) pallets for materials handling — flat pallets — part 2: performance requirements and selection of tests," (2005). https://www.iso.org/standard/34398.html.
21) A. Jha, M. Soni, and M. Suhaib, "Non-invasive invitro modelling and finite elemental analysis of a uniquely designed prosthetic hand," *Evergreen*, 9 (*3*) 729–736 (2022). doi:10.5109/4843106.
22) M.M.A. Baig, "Designing novel grooved pallets for industrial application," Cleveland State University, 2018. https://engagedscholarship.csuohio.edu/etdarchive/1104.
23) A. Waseem, A. Nawaz, N. Munir, B. Islam, and S. Noor, "Comparative analysis of different materials for pallet design using ansys," *International Journal of Mechanical and Mechatronics Engineering*, 13 (*2*) 26–32 (2013).
24) J.A. Bayona, H.A. Garnica, J.L. Luna, G.A. Juzga, and L.R. Ortiz, "Study case: evaluation of pallets manufactured by structural foam with polietilene from analysis by the finite element method and mechanical tests," *J Phys Conf Ser*, 1938 (*1*) (2021). doi:10.1088/1742-6596/1938/1/012007.
25) T. Boonsri, S. Rukchonlatee, and I. Jangchud, "Wood plastic composites (wpcs) from multilayer packaging wastes and rhdpe as pallets for green industry," *IOP Conf Ser Mater Sci Eng*, 1234 (*1*) 012022 (2022). doi:10.1088/1757-899x/1234/1/012022.
26) C. Homkhiew, T. Ratanawilai, and W. Thongruang, "The optimal formulation of recycled polypropylene/rubberwood flour composites from experiments with mixture design," *Compos B Eng*, 56 350–357 (2014). doi:10.1016/j.compositesb.2013.08.041.
27) N. S, and S. Joseph, "Application of response surface methodology for the composition optimization of polycaprolactone based composite membrane," *Indian Journal of Chemical Technology*, 29 296–302 (2022). doi:10.56042/ijct.v29i3.51344.
28) A. Usman, H. Sutanto, N. Shehu, and A. Yaro, "Response Surface Methodology Optimization in Asphalt Mixtures: A Review," in: Response Surface Methodology in Engineering Science, IntechOpen, 2021. doi:10.5772/intechopen.95994.
29) S. Bhattacharya, "Central Composite Design for Response Surface Methodology and Its Application in Pharmacy," in: Response Surface Methodology in Engineering Science, IntechOpen, 2021. doi:10.5772/intechopen.95835.
30) D.A.I. Malyuta, K.L. Matteson, M.P. Berry, D. Bajwa, and C. Ryan, "Experimental statistical modeling of tensile properties and flexural stiffness of recycled high-density polyethylene (rhdpe) thermoplastic using response surface methodology (rsm)," *Results in Materials*, 20 (2023). doi:10.1016/j.rinma.2023.100472.
31) S. Dixit, G. Mishra, and V.L. Yadav, "Optimization of novel bio-composite packaging film based on alkali-

treated hemp fiber/polyethylene/polypropylene using response surface methodology approach," *Polymer Bulletin*, 79 (*4*) 2559–2583 (2022). doi:10.1007/s00289-021-03646-5.

32) C.-S. Javier, A.-R. Sergio, Z.-G. Roberto, and D.-D. Jorge, "Optimization of the tensile and flexural strength of a wood-pet composite," *Ingeniería, Investigación y Tecnología*, 16 (*1*) 105–112 (2015). doi:10.1016/s1405-7743(15)72111-6.

33) R. V. Lenth, "Response-surface methods in r, using rsm," *J Stat Softw*, 32 (*7*) 1–17 (2009). doi:10.18637/jss.v032.i07.

34) G. Taqwatomo, D. Novriadi, B.M. Panjaitan, H. Prasetyo, Y. Subagyo, A.E. Mulyono, S. Rahayu, D.K. Arti, and O.P.A. Putra, "Mechanical Properties of Recycling Mixed Waste Plastic Predicted on Pallet Application Using Finite Element Analysis," in: E3S Web of Conferences, EDP Sciences, 2024. doi:10.1051/e3sconf/202448303019.

35) M. Arjuna Putra Perdana, A. Hapid, A. Muharam, S. Kaleg, R. Ristiana, and A. Christantho Budiman, "Crashworthiness enhancement: the optimization of vehicle crash box performance by utilizing bionic-albuca spiralis thin-walled structure," *Evergreen*, 10 (*03*) 1961–1967 (2023). doi:10.5109/7151754.

36) W. Liu, Y.J. Wang, and Z. Sun, "Effects of polyethylene-grafted maleic anhydride (pe-g-ma) on thermal properties, morphology, and tensile properties of low-density polyethylene (ldpe) and corn starch blends," *J Appl Polym Sci*, 88 (*13*) 2904–2911 (2003). doi:10.1002/app.11965.

37) F.D.O. Riswanto, A. Desra, R.M. Sari, V. Thomas, A. Rohman, S. Pramono, and S. Martono, "Employing an r software package rsm for optimizing of genistein, daidzein, and glycitein separation and its application for soy milk analysis by hplc method," *Indonesian Journal of Chemistry*, 20 (*5*) 1184–1198 (2020). doi:10.22146/ijc.51669.

38) L. Zhang, and Y. Yue, "Influence of waste glass powder usage on the properties of alkali-activated slag mortars based on response surface methodology," *Constr Build Mater*, 181 527–534 (2018). doi:10.1016/j.conbuildmat.2018.06.040.

39) M.H. Zakria, A. Jaafar, M. Ghazali, M. Nawawi, M. Rizal, and A. Rahman, "Propylene yield assessment utilizing response surface methodology for naphtha pyrolysis cracking," *Evergreen*, 10 (*01*) 608–616 (2023). doi:10.5109/6782168.

40) P. Purwono, H. Hadiyanto, and M.A. Budihardjo, "Harvesting of dunaliela salina at low concentrations using spiral electrocoagulation (sec)," *Evergreen*, 11 (*1*) 95–105 (2024). doi:10.5109/7172231.

41) R. Yadav, S. Prakash Dwivedi, and V.K. Dwivedi, "Effect of casting parameters on tensile strength of chrome containing leather waste reinforced aluminium based composite using rsm," *Evergreen*, 09 (*04*) 1031–1038 (2022). doi:10.5109/6625716.

42) K.M. Ramachandran, and C.P. Tsokos, "Goodness-of-Fit Tests Applications," in: Mathematical Statistics with Applications in R, Elsevier, 2015: pp. 371–408. doi:10.1016/b978-0-12-417113-8.00007-2.

43) M. Singh, and P.S. Bharti, "Development of models to predict flexural strength of 3d printed specimens in terms of input parameters," *Evergreen*, 11 (*2*) 1292–1298 (2024). doi:10.5109/7183438.

44) H. Dadkhah, and M.A. Behnajady, "Optimization of photooxidative removal of p-nitrophenol in a spinning disc photoreactor using response surface methodology," *Chem Eng Commun*, 206 (*3*) 398–408 (2019). doi:10.1080/00986445.2018.1494581.

45) M.A. Salman Khan, and C. Senthil Kumar, "Investigating performance of wire electric discharge machining of nimonic 90 and rsm modeling," *Evergreen*, 11 (*4*) 3099–3108 (2024). doi:10.5109/7326948.

46) R. Ratnawati, R. Wulandari, A.C. Kumoro, and H. Hadiyanto, "Response surface methodology for formulating pva/starch/ lignin biodegradable plastic," *Emerging Science Journal*, 6 (*2*) 238–255 (2022). doi:10.28991/ESJ-2022-06-02-03.

47) S.L. Fávaro, A.R. Freitas, T.A. Ganzerli, A.G.B. Pereira, A.L. Cardozo, O. Baron, E.C. Muniz, E.M. Girotto, and E. Radovanovic, "PET and aluminum recycling from multilayer food packaging using supercritical ethanol," *Journal of Supercritical Fluids*, 75 138–143 (2013). doi:10.1016/j.supflu.2012.12.015.

48) S. Choudhary, A. Sharma, K. Srivastava, H. Purohit, and M. Vats, "Read range optimization of low frequency rfid system in hostile environmental conditions by using rsm approach," *Evergreen*, 7 (*3*) 396–403 (2020). doi:10.5109/4068619.

49) N. Manocha, H. Agnihotri, M. Amir Khan, and E. Neha, "Conceptual design of 17 dof dexterous robotic hand for grasping and manipulation task," *Evergreen*, 11 (*02*) 1254–1262 (2024). doi:10.5109/7183432.

50) G. Xiang, A. Pownuk, O. Kosheleva, and S.A. Starks, "Von Mises Failure Criterion in Mechanics of Materials: How to Efficiently Use it Under Interval and Fuzzy Uncertainty," in: NAFIPS 2007 - 2007 Annual Meeting of the North American Fuzzy Information Processing Society, IEEE, San Diego, CA, USA, 2007: pp. 570–575. doi:10.1109/NAFIPS.2007.383903.

51) E.D. Purnomo, M. Azka, L. Hotma, A. Aziz, K. Herbandono, Nasril, and Arifin, "The prediction of stress and safety factor of shock absorber based on cyclic loading using finite element method," *Evergreen*, 10 (*4*) 2456–2463 (2023). doi:10.5109/7162006.

52) C. Quesenberry, L. Horvath, J. Bouldin, and M.S. White, "The effect of pallet top deck stiffness on the compression strength of asymmetrically supported corrugated boxes," *Packaging Technology and*

Science, 33 (*12*) 547–558 (2020). doi:10.1002/pts.2533.

53) S. Piedade Cestari, P.V. Rodrigues, A.C. Ribeiro, M.C.R. Castro, V. Cruz, A.R. Torres, N. Ramos, and A.V. Machado, "Compatibilizer efficiency in enhancing marine plastic waste valorization through simulated recycled plastic blends," *Polymers (Basel)*, 16 (*23*) (2024). doi:10.3390/polym16233441.
54) F.A. Radini, R. Wulandari, S.J.A. Nasiri, and D.A. Winarto, "Performance comparison of plastic shopping bags in modern and traditional retail," in: IOP Conf Ser Mater Sci Eng, Institute of Physics Publishing, 2017. doi:10.1088/1757-899X/223/1/012058.
55) M. Djebara, J.P. Stoquert, M. Abdesselam, D. Muller, and A.C. Chami, "FTIR analysis of polyethylene terephthalate irradiated by mev he +," *Nucl Instrum Methods Phys Res B*, 274 70–77 (2012). doi:10.1016/j.nimb.2011.11.022.
56) R.S. Chen, M.H. Ab Ghani, M.N. Salleh, S. Ahmad, and S. Gan, "Influence of blend composition and compatibilizer on mechanical and morphological properties of recycled hdpe/pet blends," *Materials Sciences and Applications*, 05 (*13*) 943–952 (2014). doi:10.4236/msa.2014.513096.
57) A.A.A. ElHakim, S. Awad, M.F. Radwan, E.E. Abdel-Hady, and S.M. ElKousy, "Preparation and characterization of proton exchange membrane by uv photografting technique," *Journal of Solid State Electrochemistry*, 23 (*10*) 2813–2824 (2019). doi:10.1007/s10008-019-04388-1.